A Tetraorganyl-Alumaborane with An Al–B σ-Bond and Two Adjacent Lewis-Acidic Centers

Satoshi Kurumada, Makoto Yamashita*

Department of Molecular and Macromolecular Chemistry, Graduate School of Engineering, Nagoya University, Furo-cho, Chikusa-ku, Nagoya, Aichi 464-8603, Japan

ABSTRACT: A tetraorganyl-alumaborane (**3**) that contains an Al–B bond and twisted Al and B planes was synthesized and structurally characterized. UV-vis absorption spectroscopy, electrochemical measurement, and DFT calculations were employed to reveal the electronic properties of **3**. The reactivity of the **3** toward DMSO and CO was studied to demonstrate its deoxygenating abilities. Based on the results of the DFT calculations, a detailed reaction mechanism was developed, which highlighted the important role of the distinct Lewis acidity of the group-13 elements Al and B in **3**.

Neutral tricoordinate boron and aluminum compounds are widely used in organic synthesis as Lewis-acidic catalysts. Their Lewis acidity, which arises from a vacant p-orbital, is generally weakened by substitution with π-electron-donating group(s), the coordination of a Lewis base, or the formation of a 3-center-2-electron bond to satisfy the octet rule.[1] Accordingly, carbon-substituted boron and aluminum compounds without such stabilizing effects exhibit unperturbed Lewis acidity. In contrast, we have recently reported enhancement of the Lewis acidity of the boron atoms in pinB–$BMes_2$ (pin = pinacolato; Mes = 2,4,6-$Me_3C_6H_2$) by overlapping the two vacant p-orbitals of two boron atoms.[2] This concept was expanded to an all carbon-substituted diborane(4) (**A**; Figure 1), which exhibited even higher Lewis acidity than the corresponding triarylborane and pinB–$BMes_2$.[2-3] Similar carbon-substituted homodinuclear species **B**–**E** with a B–B or Al–Al single bond have also been synthesized,[4-8] although their Lewis acidity has not been reported. In contrast, the hitherto reported heterodinuclear alumaboranes **F**–**I**[9-12] are electronically stabilized by either π-electron-donating group(s), the coordination of a Lewis base, or the formation of a 3-center-2-electron bond. Thus, electronically unperturbed heterodinuclear B–Al species have not been reported so far.

The Lewis acidity of boron and aluminum compounds is controlled by several factors. In comparison, boron compounds have a higher electron affinity due to the lower energy level of the 2p-orbital on the boron atom,[13] whereas longer Al–X bonds in aluminum compounds lead to less steric congestion around the aluminum atom upon complexation with a Lewis base. The reported fluoride ion affinity (FIA), a computationally obtained indicator for evaluating Lewis acidity, of 59.2 kcal/mol for BMe_3 and 88.1 kcal/mol for $AlMe_3$ indicate that $AlMe_3$ behaves as a stronger Lewis acid toward the fluoride ion than BMe_3.[14] In this case, it is thought that the electropositive Al atom[15] interacts strongly with the negatively charged fluoride ion. In other words, Coulomb interactions can also be a factor in determining Lewis acidity. Thus, it would be interesting to examine how alumaboranes, which contain two different Lewis acidic centers, behave toward Lewis bases.

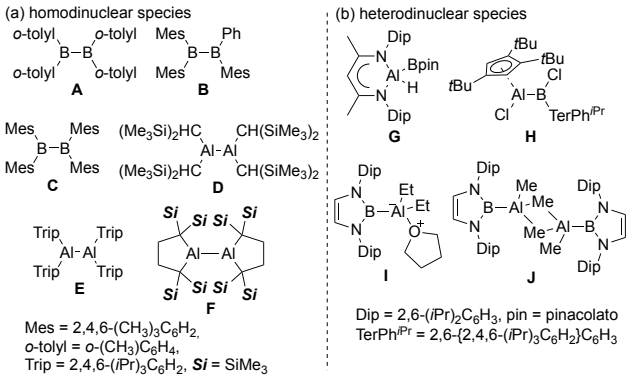

Figure 1. Previously reported singly-bonded dinuclear boron and aluminum species having (a) tetraorganyl homodinuclear structures, and (b) electronically stabilized heterodinuclear structures.

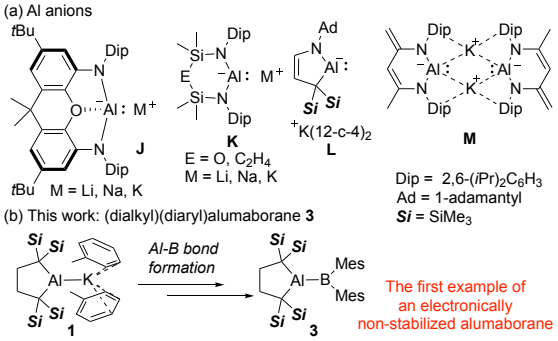

Figure 2. (a) Al(I) anions that have been reported to serve as nucleophilic Al reagents. (b) This work: Synthesis of (dialkyl)(diaryl)alumaborane **3** by using dialkyl-Al(I) anion **1**.

Recently, Al(I) anions **J**–**M** and **1** have been reported as nucleophilic Al reagents that undergo nucleophilic substitution, addition, cycloaddition, and transmetalation reactions (Figure 2a).[8,16-23] Among these, dialkylalumanyl anion **1**[8] is the only reagent that can introduce an non-heteroatom-substituted alumanyl

substituents.[20-23] Herein, we report the synthesis of a tetraorganylalumaborane (**3**) (Figure 2b) together with its physical properties and reactivity.

The alumaborane **3** was synthesized as illustrated in Scheme 1. The reaction of **1** with dimesitylfluoroborane furnished borylfluoroaluminate **2** as red crystals through the migration of fluoride from boron to aluminum.[24] Subsequently, **2** was treated with Me_3SiOTf to remove the fluoride to afford yellow crystalline alumaborane **3**. The crystal structures of **2** and **3** are shown in Figure 3. The Al–B bonds in **2** [2.2805(19) Å] and **3** [2.191(2) Å] are longer than those of all previously reported alumaboranes [2.119(3)–2.156(2) Å],[9-12] probably due to the steric repulsion between the bulky trimethylsilyl and mesityl groups. The shorter Al–B bond in **3** compared to that in **2** reflects the change in hybridization at the aluminum atom. In the structure of **3**, planar and trigonal Al and B atoms are observed (angle sum around Al and B = 360°) with highly twisted Al and B planes (C–Al–B–C = −60.5°). The ^{1}H NMR spectrum of **2** indicates a C_s-symmetrical structure. A broad ^{19}F NMR signal at 139 ppm ($h_{1/2}$ = 251 Hz) and a low-field ^{11}B NMR signal at δ_B 122 ppm corroborate the binding of fluoride to aluminum in solution, as was observed in the solid state.[8, 25] In contrast, the ^{1}H NMR spectrum of **3** exhibited a C_{2v}-symmetrical pattern and the ^{11}B NMR signal of **3** resonated at δ_B 109 ppm, which suggests the existence of the planarized aluminum and boron atoms in solution.

Scheme 1. Synthesis of alumaborane 3.

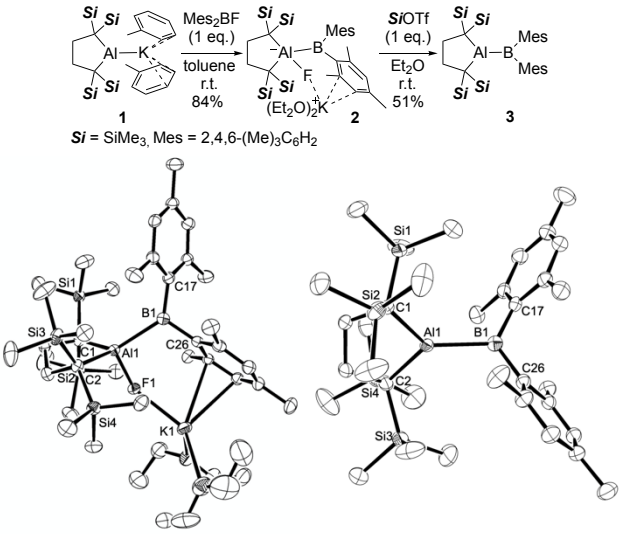

Figure 3. Molecular structures of **2** (left) and **3** (right) with thermal ellipsoids at 50% probability; all hydrogen atoms are omitted for clarity. For a summary of the metrical parameters, see Table S2.

The electronic structure of **3** was examined using UV-vis absorption spectroscopy, electrochemistry, DFT calculations, and natural-bond-orbital (NBO) analysis. The UV-Vis spectrum of **3** in hexane exhibited an absorption maximum at 452 nm (ε = 3370), which is reflected in the yellow color of **3**, whereas the emission spectrum showed a weak emission (λ_{ex} = 475 nm; λ_{max} = 552 nm; Φ = 0.010) (Figures S17, S18). Similar to our previous reports on diborane(4) **A**,[2b,3a] the dependence of the LUMO energy level and the electronic energy on the C–Al–B–C torsion angle of **3** was estimated using DFT calculations; the results are presented in Figure 4a, along with those for **A**. While **A** has the lowest LUMO level at a torsion angle of 0°, **3** has the lowest LUMO level (−1.34 eV) at −20°, and its lowest value is less negative than that of **A** (−2.20 eV). This is consistent with the differential pulse voltammetry (DPV) of **3**, which exhibits a reduction peak at −2.32 V (vs. Cp_2Fe/Cp_2Fe^+); this value is slightly more negative than that of **A** (−2.11 V) (Figure S20). The maximum energy change for **3** was estimated to be ca. 4 kcal/mol between the C–Al–B–C torsion angles of −61.9° and −30°, indicating free rotation of the Al–B bond. Some key molecular orbitals of **3** at torsion angles of −61.9° and −20° are summarized in Figure 4b. Based on the difference in energy between the 2p and 3p orbitals, the LUMO at −61.9° mainly consists of the 2p orbital of the B atom and the π^*-orbitals of the two mesityl rings. In contrast, the contribution of the 3p orbital of the Al atom is significant in the LUMO+1. At a torsion angle of −20.0°, the LUMO corresponds to the two completely merged vacant p-orbitals on the Al and B atoms. In both states, the Al–B bond significantly contributes to the HOMO. TD-DFT calculations suggested that the characteristic visible absorption of **3** corresponds to the HOMO–LUMO transition (Table S2, Figures S23, S24). The natural population analysis (NPA) charges of +1.82 on Al and +0.14 on B suggest polarization of the Al(δ^+)–B(δ^-) bond due to the difference in the electronegativity of them. The second-order perturbation energy in the NBO analysis showed that the negative hyperconjugation from the Si-C σ-bonds to the vacant 3p-orbital of Al (<20 kcal/mol) and the π-donation from the two Mes substituents to the vacant 2p-orbital of B (<9 kcal/mol) are weaker than the binding of fluoride to $AlMe_3$ (FIA: 88.1 kcal/mol).[14]

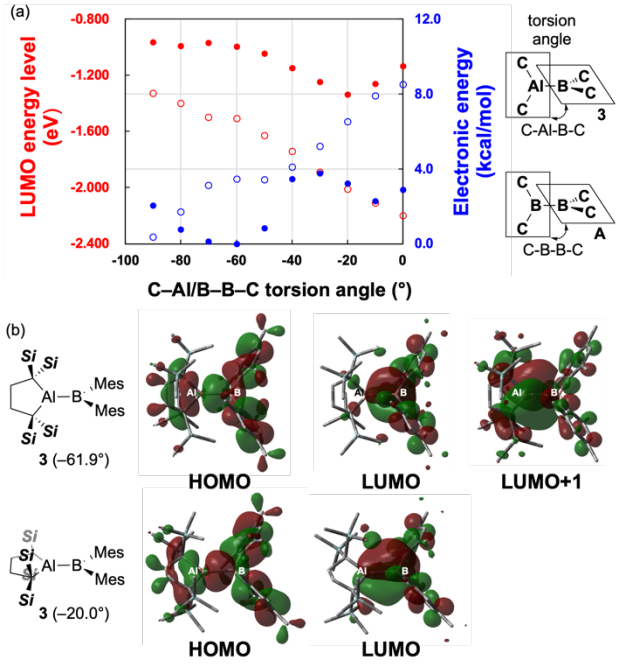

Figure 4. (a) Dependence of the LUMO energy level (red; in eV) and the relative stability (blue; in kcal/mol) of **3** (full circles) and **A** (open circles) on the torsion angle of the C–E–B–C moiety. (b) Frontier orbitals of the rotational isomers of **3** at C–Al–B–C = −61.9° (top) and C–Al–B–C = −20.0° (bottom).

Subsequently, the reactivity of **3** toward small molecules was examined (Scheme 2). The reaction of **3** with Me_2S^+–O^- led to the formation of boroxyalumane **4** and dimethyl sulfide[26] in the same manner as the reaction of dialumane **D**.[27] The ^{1}H NMR spectrum of **4** exhibited a C_{2v}-symmetrical pattern, and the ^{11}B NMR signal of **4**

was observed at a relatively low-field (δ_B 49 ppm), supporting the existence of the B-O bond in **4**. A single-crystal X-ray diffraction analysis revealed a linear Al–O–B structure with twisted Al and B planes (Figure S21). On the other hand, the reaction of **3** with CO afforded benzocyclobutane-substituted Al–O–B species **5** [Scheme 3(a)], in which the C≡O triple bond of CO[28] and the benzylic C–H bond of the Mes group were cleaved, which was supported by a preliminary crystallographic analysis (Figure S22; R_1 = 12%).[29] The five non-equivalent signals of the Me groups in the Mes substituents, and the one methine and one methylene signals in the ^{1}H NMR spectrum of **5** support the C-H cleavage of one Me group. Moreover, the ^{11}B NMR signal at high-field (δ_B 51 ppm) supports the binding of the oxygen atom to the boron atom.

Scheme 2. Reactivity of 3 toward small molecules.

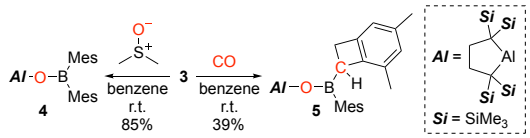

DFT calculations at the M06-2X/6-31+G(d)/PCM (SMD, Benzene) level of theory were used to shed light on the details of the mechanism by which **4** is produced from **3** and Me_2S^+–O^-. A schematic illustration of the mechanism and its energy profile are provided in Scheme 3. Two possible intermediates, **int_6** and **int_7**, were found, in which the negatively charged oxygen atom of Me_2S^+–O^- binds to Al and B atoms to form a four-coordinate aluminate or borate structure. The subsequent 1,2-B-shift from **int_6** and 1,2-Al-shift from **int_7** afford the same product (**4**) via $\mathbf{TS_{6\text{-}4}}$ and $\mathbf{TS_{7\text{-}4}}$, in which the migrating boryl or alumanyl group nucleophilically attacks the O atom with concomitant elimination of dimethyl sulfide. The pathway via **int_6** and $\mathbf{TS_{6\text{-}4}}$ has a lower activation energy than that via **int_7** and $\mathbf{TS_{7\text{-}4}}$. These results suggest that the Coulomb interaction between the electropositive Al atom and the negatively charged O atom can be expected to contribute to the energetically lower pathway, which is consistent with the preference of the fluoride for the Al atom rather than the B atom in **2**.

Scheme 3. (a) Schematic illustration of the DFT-based reaction mechanism for the formation of 4 from 3; (b) energy profile.

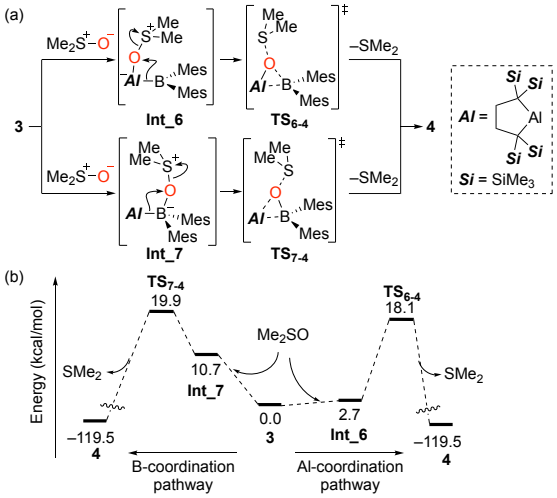

A schematic representation of the DFT-based mechanism and its energy profile for the reaction of **3** with CO to form **5** is summarized in Scheme 4. Coordination of CO to **3** generates four-coordinate borate intermediate **Int_8**, in which the carbon atom of CO binds to the B atom. A subsequent 1,2-shift of the R_2Al moiety to the C atom of CO furnishes the second intermediate, O--Al interacting (alumanyl)(boryl)ketone **Int_9** via $\mathbf{TS_{8\text{-}9}}$ with an activation energy of 4.3 kcal/mol. It is feasible to assume another pathway via four-coordinate aluminate intermediate **Int_11** and O--B interacting (alumanyl)(boryl)ketone intermediate **Int_12**. However, these intermediates are less stable than **Int_8** and **Int_9**. These results stand in stark contrast to the reaction of **3** with Me_2S^+–O^-, which is initiated by O--Al interaction (Scheme 3). These results indicate two characteristics: (i) The relative stability between **Int_8** and **Int_11** is controlled by orbital interactions. i.e., the lone pair on the C atom of CO interacts with the vacant 2p orbital on the B atom in **Int_8** more strongly than with the 3p orbital on the Al atom in **Int_11**. (ii) The Coulomb interactions control the relative stability between **Int_9** and **Int_12**), i.e., the electronegative O atom of the carbonyl group interacts with the electropositive Al atom in **Int_9** more strongly than with the B atom in **Int_12**. The strained structure of **Int_9** induces the cleavage of the Al–C bond to afford boraoxaallene **Int_10** with a negligible barrier,[30] which further undergoes a 1,2-Mes-shift to furnish boraalkene **Int_13** via $\mathbf{TS_{10\text{-}13}}$. The alumoxy group in **Int_13** migrates to the boron atom with assistance from the π-electrons of the Mes group to give borataallene **Int_14** with concomitant formation of a thermodynamically stable B–O bond.[31] Since **Int_14** can be expected to contain a contribution from (aryl)(boryl)carbene, the C atom of **Int_14** deprotonates the benzylic C–H to generate *ortho*-quinodimethane **Int_15** via the highest activation energy in this profile (21.1 kcal/mol). The subsequent aromatizing electrocyclic reaction of **Int_15** results in the formation of **5**. Thus, the distinct characteristic Lewis acidity of the B and Al atoms, with the former preferring orbital interaction and the latter favoring Coulomb interaction, would be responsible for the present characteristic pathway to form **5**.

Scheme 4. (a) Schematic illustration of the DFT-based reaction mechanism for the formation of 5 from 3; (b) energy profile.

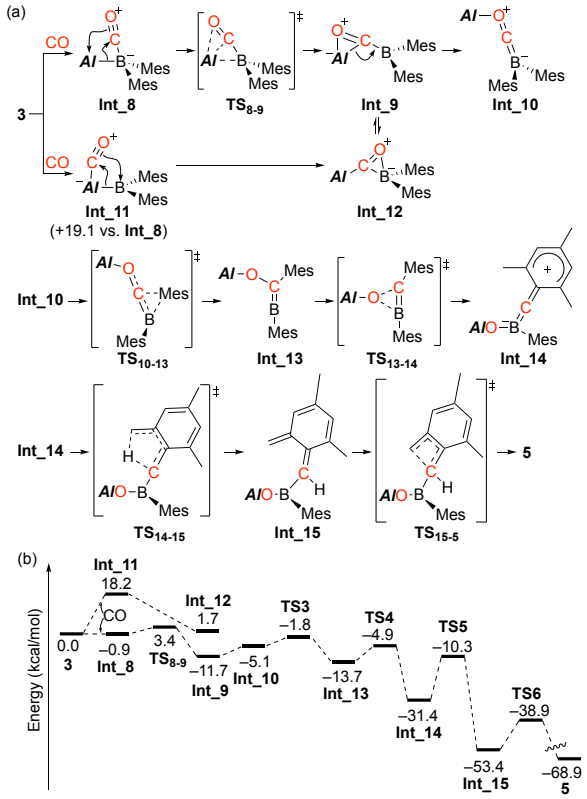

In summary, compound **3**, which contains an Al–B bond, was synthesized as the first example of a tetraorganyl-alumaborane. The structure of **3**, which consists of dihedral Al and B-containing planes, was determined via a crystallographic study. The electronic character arising from the Al–B bond of **3** was estimated experimentally using absorption spectroscopy and electrochemistry as well as theoretically using DFT calculations. The reaction of **3** with DMSO and CO gave two different Al–O–B bonded species. An analysis of the reaction mechanism using DFT calculations revealed the importance of the distinct Lewis acidity of the group-13 elements Al and B in **3**.

ASSOCIATED CONTENT

Supporting Information

The Supporting Information is available free of charge on the ACS Publications website.

Experimental and computational details (PDF)

Crystallographic data for **2**-**5** (CIF)

DFT coordinates (XYZ)

AUTHOR INFORMATION

Corresponding Author

* makoto@oec.chembio.nagoya-u.ac.jp

Notes

The authors declare no competing financial interest.

ACKNOWLEDGMENTS

This research was supported by a Grant-in-Aid for Scientific Research (B) (JSPS KAKENHI grant 21H01915). S.T. is grateful for a JSPS research fellowship (202115731). Theoretical calculations were carried out using resources at the Research Center for Computational Science (Okazaki).

REFERENCES AND NOTES

1. Lewis, G. N., Valence and the Structure of Atoms and Molecules. Chemical Catalogue Company, Inc.: New York, 1923.

2. (a) Asakawa, H.; Lee, K.-H.; Lin, Z.; Yamashita, M., Facile scission of isonitrile carbon–nitrogen triple bond using a diborane(4) reagent. *Nat. Commun.* **2014**, *5*, 4245. (b) Asakawa, H. Lee, K.-H.; Furukawa, K.; Lin, Z.; Yamashita, M., Lowering Reduction Potential of Boron Compound by Substituent Effect of Boryl Group: One-Electron Reduction of Unsymmetrical Diborane(4), *Chem. Eur. J.* **2015,** *21*, 4267-4271. (c) Katsuma, Y.; Asakawa, H.; Lee, K.-H.; Lin, Z.; Yamashita, M., Ring Contraction of Pinacolatoboryl Group to Form 1,2-Oxaboretane Ring: Reaction of Unsymmetrical Diborane(4) with 2,6-Dimethylphenylisocyanide, *Organometallics* **2016,** *35*, 2563-2566. (d) Katsuma, Y.; Asakawa, H.; Yamashita, M., Reactivity of Highly Lewis Acidic Diborane(4) towards Pyridine and Isocyanide: Formation of Boraalkene-Pyridine Complex and *ortho*-Functionalized Pyridine Derivatives, *Chem. Sci.* **2018,** *9*, 1301-1310.

3. (a) Tsukahara, N.; Asakawa, H.; Lee, K.-H.; Lin, Z.; Yamashita, M., Cleaving Dihydrogen with Tetra(*o*-tolyl)diborane(4). *J. Am. Chem. Soc.* **2017**, *139*, 2593-2596. (b) Katsuma, Y.; Tsukahara, N.; Wu, L.; Lin, Z.; Yamashita, M., Reaction of $B_2(o\text{-tol})_4$ with CO and Isocyanides: Cleavage of the C≡O Triple Bond and Direct C-H Borylations, *Angew. Chem. Int. Ed.* **2018,** *57*, 6109-6114.

4. Moezzi, A.; Olmstead, M. M.; Bartlett, R. A.; Power, P. P. Enhanced Thermal Stability in Organodiborane(4) Compounds: Synthesis and Structural Characterization of MeO(Mes)BB(Mes)OMe, $Mes_2BB(Mes)OMe$, $Mes_2BB(Mes)Ph$, and $Mes_2BB(Mes)CH_2SiMe_3$ (Mes = 2,4,6-$Me_3C_6H_2$). *Organometallics* **1992**, *11*, 2383–2388.

5. Shoji, Y.; Tanaka, N.; Ikabata, Y.; Sakai, H.; Hasobe, T.; Koch, N.; Nakai, H.; Fukushima, T., Tetraaryldiborane(4) Can Emit Dual Fluorescence Responding to the Structural Change around the B-B Bond, *Angew. Chem. Int. Ed.* **2022**, *61*, e202113549.

6. Uhl, W. Tetrakis[Bis(Trimethylsilyl)Methyl]Dialan(4), Eine Verbindung Mit Aluminium–Aluminium-Bindung. *Z. Naturforsch*, **1988**, *43b*, 1113–1118.

7. Wehmschulte, R. J.; Ruhlandt-Senge, K.; Olmstead, M. M.; Hope, H.; Sturgeon, B. E.; Power, P. P. Reduction of a Tetraaryldialane to Generate Aluminum-Aluminum π-Bonding. *Inorg. Chem.* **1993**, *32*, 2983–2984.

8. Kurumada, S.; Takamori, S.; Yamashita, M. An alkyl-substituted aluminium anion with strong basicity and nucleophilicity. *Nat. Chem.* **2020,** *12*, 36-39.

9. Wiberg, N.; Amelunxen, K.; Blank, T.; Nöth, H.; Knizek, J., Tetrasupersilyldialuminum $[(t\text{-Bu})_3Si]_2Al\text{–}Al[Si(t\text{-Bu})_3]_2$: The Dialane(4) with the Longest Al–Al Bond to Date. *Organometallics* **1998**, *17*, 5431-5433.

10. Chu, T.; Korobkov, I.; Nikonov, G. I., Oxidative Addition of σ Bonds to an Al(I) Center. *J. Am. Chem. Soc.* **2014**, *136*, 9195-9202.

11. Hofmann, A.; Pranckevicius, C.; Tröster, T.; Braunschweig, H., Aluminum(I)/Boron(III) Redox Reactions. *Angew. Chem. Int. Ed.* **2019**, *58*, 3625-3629.

12. (a) Dettenrieder, N.; Dietrich, H. M.; Schädle, C.; Maichle-Mössmer, C.; Törnroos, K. W.; Anwander, R., Organoaluminum Boryl Complexes. *Angew. Chem. Int. Ed.* **2012**, *51*, 4461-4465; (b) Dettenrieder, N.; Schädle, C.; Maichle-Mössmer, C.; Anwander, R., Reactivity of boryllithium with $AlMe_3$, $AlEt_3$, and $GaMe_3$, including the synthesis of a lanthanum heterogallate complex. *Dalton Trans.* **2014**, *43*, 15760-15770.

13. Schulz, A.; Kaim, W. Bor-organische Redoxsysteme. Chem. Ber. 1989, 122, 1863-1868.

14. Erdmann,P.; Leitner, J.; Schwarz, J.; Greb, L., An Extensive Set of Accurate Fluoride Ion Affinities for p-Block Element Lewis Acids and Basic Design Principles for Strong Fluoride Ion Acceptors. *ChemPhysChem* **2020**, *21*, 987-994.

15. Emsley, J., *The Elements*. 3rd ed.; Oxford University Press: New York, 1998.

16. (a) Hicks, J.; Vasko, P.; Goicoechea, J. M.; Aldridge, S., Synthesis, structure and reaction chemistry of a nucleophilic aluminyl anion. *Nature* **2018**, *557*, 92-95; (b) Hicks, J.; Vasko, P.; Goicoechea, J. M.; Aldridge, S., Reversible, Room-Temperature C–C Bond Activation of Benzene by an Isolable Metal Complex. *J. Am. Chem. Soc.* **2019**, *141*, 11000-11003; (c) Hicks, J.; Mansikkamäki, A.; Vasko, P.; Goicoechea, J. M.; Aldridge, S., A nucleophilic gold complex. *Nat. Chem.* **2019**, *11*, 237-241; (d) Hicks, J.; Heilmann, A.; Vasko, P.; Goicoechea, J. M.; Aldridge, S., Trapping and Reactivity of a Molecular Aluminium Oxide Ion. *Angew. Chem. Int. Ed.* **2019**, *58*, 17265-17268; (e) Hicks, J.; Vasko, P.; Heilmann, A.; Goicoechea, J.; Aldridge, S., Arene C–H activation at aluminium(I): *meta* selectivity driven by the electronics of S_NAr chemistry. *Angew. Chem. Int. Ed.* **2020**, *59*, 20376-20380.

17. (a) Schwamm, R. J.; Anker, M. D.; Lein, M.; Coles, M. P. Reduction vs. Addition: The Reaction of an Aluminyl Anion with 1,3,5,7-Cyclooctatetraene. *Angew. Chem. Int. Ed.* **2019,** *58*, 1489-1493; (b) Anker, M. D.; Coles, M. P., Isoelectronic Aluminium Analogues of Carbonyl and Dioxirane Moieties. *Angew. Chem. Int. Ed.* **2019**, *58*, 13452-13455; (c) Anker, M. D.; Coles, M. P., Aluminium-Mediated Carbon Dioxide Reduction by an Isolated Monoalumoxane Anion. *Angew. Chem. Int. Ed.* **2019**, *58*, 18261-18265; (d) Anker, M. D.; Schwamm, R. J.; Coles, M. P. Synthesis and reactivity of a terminal aluminium–imide bond. *Chem. Commun.* **2020,** *56*, 2288-2291; (e) Anker, M. D.; McMullin, C. L.; Rajabi, N. A.; Coles, M. P., Carbon–Carbon Bond Forming Reactions Promoted by Aluminyl and Alumoxane Anions: Introducing the Ethenetetraolate Ligand. *Angew. Chem. Int. Ed.* **2020**, *59*, 12806-12810.

18. Schwamm, R. J.; Coles, M. P.; Hill, M. S.; Mahon, M. F.; McMullin, C. L.; Rajabi, N. A.; Wilson, A. S. S., A Stable Calcium Alumanyl. *Angew. Chem. Int. Ed.* **2020**, *59*, 3928-3932.

19. (a) Koshino, K.; Kinjo, R., Construction of σ-Aromatic AlB_2 Ring via Borane Coupling with a Dicoordinate Cyclic (Alkyl)(Amino)Aluminyl Anion. *J. Am. Chem. Soc.* **2020**, *142*, 9057-9062. (b) Koshino, K.; Kinjo, R., Fragmentation of White Phosphorus by a Cyclic (Alkyl)(Amino)Alumanyl Anion. *Organometallics* **2020**, *39*, 4183-4186.

20. Grams, S.; Eyselein, J.; Langer, J.; Färber, C.; Harder, S., Boosting Low Valent Al(I) Reactivity with a Potassium Reagent. *Angew. Chem. Int. Ed.* **2020**, *59*, 15982-15986.

21. Sugita, K.; Nakano, R.; Yamashita, M., Cycloaddition of Dialkylalumanyl Anion toward Unsaturated Hydrocarbons in (1+2) and (1+4) Modes. *Chem. Eur. J.* **2020**, *26*, 2174-2177.

22. Sugita, K.; Yamashita, M., An Alumanylyttrium Complex with an Absorption due to a Transition from the Al–Y Bond to an Unoccupied d-Orbital. *Chem. Eur. J.* **2020,** *26*, 4520-4523.

23. Kurumada, S.; Sugita, K.; Nakano, R.; Yamashita, M., A meta-Selective C-H Alumination of Mono-Substituted Benzene by Using An Alkyl-Substituted Al Anion through Hydride-Eliminating S_NAr Reaction *Angew. Chem. Int. Ed.* **2020**, *59*, 20381-20384.

24. Considering the potential reactivity of **2** as a boryl-anion equivalent, **2** was treated with several other electrophiles (e.g., MeOTf, acyl chloride, aryl bromide, and aryl fluoride). However, these reactions resulted either in the defluorination of **2** to furnish alumaborane **3** or in the decomposition of **2** to generate unknown products which could not be assigned to specific borylated compounds.

25. Similarly broadened ^{19}F NMR signals were observed for (triorgano)(fluoro)aluminate. See ref 8 and (a) Kopp, M. R.; Kräuter, T.; Werner, B.; Neumüller, B., CsF als Fluoridierungsmittel für Organometall-Verbindungen der Elemente der Gruppe 13. *Z. Anorg. Allg. Chem.* **1998**, *624*, 881-886; (b) Agarwal, A.; Chauhan, P. M. S., Convenient Dimethylamino Amination in Heterocycles and Aromatics with Dimethylformamide. *Syn. Commun.* **2004**, *34*, 2925-2930; (c) Ménard, G.; Tran, L.; Stephan, D. W., Activation of H_2 using P/Al based frustrated Lewis pairs and reactions with olefins. *Dalton Trans.* **2013**, *42*, 13685-13691.

26. The formation of dimethyl sulfide was confirmed using ^1H NMR spectroscopy.

27. (1) Uhl, W.; Koch, M.; Hiller, W.; Heckel, M. Tetrakis[Bis(Trimethylsilyl)Methyl]Dialuminoxane with a Linear Al–O–Al Group. *Angew. Chem. Int. Ed.* **1995**, *34*, 989–990.

28. Some C≡O triple bond cleavage reactions using main group element compounds have been reported. (i) Reaction with one component: (a) Majumdar, M.; Omlor, I.; Yildiz, C. B.; Azizoglu, A.; Huch, V.; Scheschkewitz, D. Reductive Cleavage of Carbon Monoxide by a Disilenide. A *Angew. Chem. Int. Ed.* **2015**, *54*, 8746–8750; (b) Devillard, M.; de Bruin, B.; Siegler, M. A.; van der Vlugt, J. I. Transition-Metal-Free Cleavage of CO. *Chem. Eur. J.* **2017**, *23*, 13628–13632; (c) Arrowsmith, M.; Böhnke, J.; Braunschweig,H.; Celik, A. M. Reactivity of a Dihydrodiborene with CO: Coordination, Insertion, Cleavage, and Spontaneous Formation of a Cyclic Alkyne. *Angew. Chem., Int. Ed.***2017**, *56*, 14287–14292; (d) Wang, H.; Wu, L.; Lin, Z.; Xie, Z. Transition-Metal-Like Behavior of Monovalent Boron Compounds: Reduction, Migration, and Complete Cleavage of CO at a Boron Center. *Angew. Chem. Int. Ed.* **2018**, *57*, 8708–8713; (e) Katsuma, Y.; Tsukahara, N.; Wu, L.; Lin, Z.; Yamashita, M., Reaction of $B_2(o\text{-tol})_4$ with CO and Isocyanides: Cleavage of the C≡O Triple Bond and Direct C-H Borylations. *Angew. Chem. Int. Ed.* **2018**, *57*, 6109-6114; (f) Wang, Y.; Kostenko, A.; Hadlington, T. J.; Luecke, M.-P.; Yao, S.; Driess, M. Silicon-Mediated Selective Homo- and Heterocoupling of Carbon Monoxide. *J. Am. Chem. Soc.* **2019**, *141*, 626–634; (g) Manankandayalage, C. P.; Unruh, D. K.; Krempner, C. Carbon Monoxide Bond Cleavage Mediated by an Intramolecular Frustrated Lewis Pair: Access to New B/N Heterocycles via Selective Incorporation of Single Carbon Atoms. *Chem. Commun.* **2021**, *57*, 12528–12531. (ii) Reaction with two components: (h) Dobrovetsky, R.; Stephan, D. W. Stoichiometric Metal-Free Reduction of CO in Syn-Gas. *J. Am. Chem. Soc.* **2013**, *135*, 4974–4977.; (i) . Sajid, M.; Kehr, G.; Daniliuc, C. G.; Erker, G. Formylborane Formation with Frustrated Lewis Pair Templates. *Angew. Chem. Int. Ed.* **2014**, *53*, 1118–1121. (j) Xu, M.; Kooij, B.; Wang, T.; Lin, J. H.; Qu, Z.-W.; Grimme, S.; Stephan, D. W. Facile Synthesis of Cyanide and Isocyanides from CO. *Angew. Chem. Int. Ed.* **2021**, *60*, 16965–16969. (k) Fujimori, S.; Inoue, S. Carbon Monoxide in Main-Group Chemistry. *J. Am. Chem. Soc.* **2022,** *144*, 2034-2050.

29. In spite of repeated trials for the recrystallization of **5**, only twinned crystals consisting of thin-plates were obtained.

30. The difference in activation energy between **Int_9** and **Int_10** would be very small because it is mainly based on the change in the C–O–Al angle. Therefore, it was very difficult to locate the exact transition state.

31. Considering that both the C and O atoms are incorporated in **5**, and that the C atom is inserted into the B–C bond in **3**, unlike in the reaction of **A** with CO,[3b] the mechanism for the reaction of **3** with CO should be different from that of **A** with CO. The key step is the reaction of boraalkene intermediate **Int_13**. For details, see Scheme S1 in the SI.

TOC Graphic

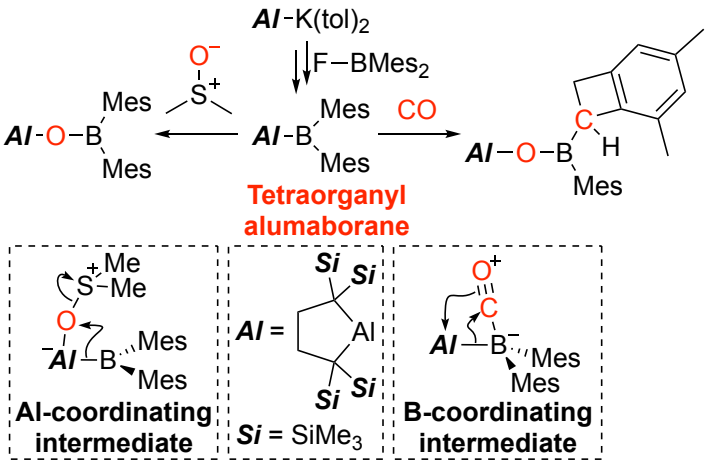
Al-K(tol)2
F–BMes2
CO
Tetraorganyl alumaborane
Al-coordinating intermediate
Si = SiMe3
B-coordinating intermediate